

Modelling longshore sediment transport under asymmetric waves*

OCEANOLOGIA, 48 (3), 2006.
pp. 395–412.

© 2006, by Institute of
Oceanology PAS.

KEYWORDS

Wave asymmetry
Wave-current interaction
Longshore
sediment transport

RAFAL OSTROWSKI
MAREK SZMYTKIEWICZ

Institute of Hydroengineering,
Polish Academy of Sciences,
(IBW PAN),
Kościerska 7, PL-80-328 Gdańsk, Poland;
e-mail: rafi@ibwpan.gda.pl

Received 8 March 2006, revised 30 July 2006, accepted 2 August 2006.

Abstract

Two wave theories are applied in calculations of longshore sediment transport rates: the second Stokes approximation and the cnoidal theory. These approaches are used to model sand motion in nearshore locations beyond and within the surf zone. Wave-current interaction in the nearbed layer and bed shear stresses are solved using a momentum integral method, whereas sediment transport is described by a three-layer model encompassing bedload, contact load and suspended load. Computational results for asymmetric waves are compared with the results obtained using linear wave theory and the conventional sediment transport models of Bailard (1981), Bijker (1971) and Van Rijn (1993).

1. Introduction

Coastal zones built of sandy sediment are subject to continuous evolution as a result of frequently changing hydrodynamic conditions. This morphodynamic evolution can be observed on many time scales and leads

* The financial support of this study by the Ministry of Science and Higher Education, Poland, under programme 2 IBW PAN is gratefully acknowledged.

to changes in both the short (hours and days) and the long term (years and decades).

Conventionally, it is assumed that seabed evolution takes place as a result of the spatial variability of net sediment transport rates. In theoretical descriptions, sediment transport is for convenience divided into cross-shore and longshore. Similarly, coastal changes in the cross-shore and longshore domains are assumed to result from the variability in the respective components of the sand's motion.

On sandy coasts, vulnerable to water flows, waves and currents elicit a quick response on the part of the littoral system. The seabed is constantly evolving towards a state of equilibrium with respect to instantaneous hydrodynamic conditions. In the Baltic Sea, however, these conditions seldom become steady and such an equilibrium cannot therefore be reached. In particular, the cross-shore profile can never take on a permanent shape, changing significantly even on short time scales (hours and days). Theoretical descriptions, numerical models and predictive simulations of this process are therefore often very difficult and unreliable. On the other hand, hindcasts and forecasts of coastal evolution in the longshore direction do very often allow distinct trends to be determined. Coastal engineering problems treated in the longshore spatial domain are thus solved with a quite high degree of accuracy and reliability. These solutions, most often obtained by the use of the so-called one-line theory for sections of the shoreline where the longshore sand motion is disturbed by coastal structures, can involve very long time scales, up to tens of years (see e.g. Szmytkiewicz et al. 2000).

In mathematical models of longshore sand transport, in contrast to the situation regarding cross-shore transport (Ostrowski 2003), wave asymmetry does not seem to be very important, because the direction of this transport is independent of wave shape. It is intuitively obvious that the transport rate will increase if the wave asymmetry does so. Because of the highly non-linear relation between hydrodynamic forcing and sediment transport, a much higher contribution of sediment transport can be expected in the wave crest phase (sediment motion in accordance with the longshore current) than in the wave trough phase (sediment motion in the opposite direction).

Presumably, then, the greater the wave asymmetry, the more intensive the longshore sediment transport. The present study was undertaken to find out what qualitative increase in the longshore sediment transport rate can be expected when asymmetric waves (with short, high crests and long, shallow troughs) are taken into consideration; Ostrowski (2002) did likewise with respect to cross-shore transport.

In the present study, the classical deterministic modelling approach is followed, which comprises a theoretical description of the physical

processes occurring in a coastal zone. Within this modelling system, wave transformation and breaking are first determined, along with wave-induced currents, which are quantitatively closely dependent on the features of the cross-shore profile. Then, sea bed roughness and bed shear stresses are calculated, from which the longshore sediment transport can be found.

The net longshore sediment transport rate at a point in the nearshore zone can be expected to depend on the bed shear stress resulting from the interaction of waves and the longshore current. This current, like most wave-driven water motions, is modelled in the phase-averaged mode. The calculations of the longshore current are based on a phase-averaged wave field and have the same or a very similar degree of accuracy. At a local point, however, where the specific water depth and wave parameters are known from the phase-averaged model, the asymmetric shape of the wave-induced nearbed velocity can be described by a wave theory appropriate to the wave regime. Non-linear superposition of the asymmetric wave-induced velocities and the steady longshore flow in the bed boundary layer yields the resultant nearbed sediment flux at the point under consideration. The rate of the net sediment transport in the upper layer of the water column also results from the solution of the wave-current bed boundary layer.

Hence, the bed boundary layer at a point on the cross-shore profile, the bed shear stresses and the sediment transport rates are determined in the phase-resolving mode, yielding instantaneous values for the entire wave period. By integrating the sediment transport rates over the wave period in the individual locations of the cross-shore profile, the authors obtained the net sand transport rates.

The above compound way of modelling, comprising phase-averaged coastal hydrodynamics and a phase-resolving sediment transport module, together constitute the quasi-phase-resolving approach.

2. Theoretical background

2.1. Wave transformation and longshore current

Coastal hydrodynamics is the force driving sediment transport processes. A reliable description of the wave-current field is crucial for a precise determination of sediment transport rates. The set of models by Szmytkiewicz (1995) and Szmytkiewicz (2002a,b), enabling calculations of wave transformation and wave-driven currents, has been validated thoroughly using laboratory and field data, both from the literature and the IBW PAN experimental facilities, namely the wave flume and the Coastal Research Station (CRS) at Lubiatowo, Poland. A brief description of this

computational framework, adapted to the purposes of the present study, now follows.

In computations of wave motion, following Battjes & Janssen (1978), it is assumed that waves are random and that their heights in the entire coastal zone can be described by a Rayleigh distribution. The wave height H is computed from the energy flux conservation equation, where the roller effect is also taken into consideration:

$$\frac{\partial}{\partial x}(E C_g \cos \theta) + \frac{\partial}{\partial x}(E_r C \cos \theta) = -D, \quad (1)$$

where E is the total wave energy, E_r the kinetic energy of the roller (as described by Svendsen 1984), C and C_g the phase and group velocity of waves, respectively, θ the wave approach angle, and D the wave energy dissipation.

In the above equation, which is a simplified form of the wave action equation, the wave energy dissipation D is calculated on the assumption that the dissipation is related to the wave breaking process only. Under this assumption, the formula of Battjes & Janssen (1978) is used:

$$D = \frac{\alpha}{4} p_b f_p \rho g H_m^2. \quad (2)$$

Their approach was successfully adapted to a multi-bar coastal zone and multiple wave breaking (Szmytkiewicz 1995).

In eq. (2), g denotes the acceleration due to gravity and ρ is the water density; the factor p_b , characterising the percentage of broken and breaking waves at a given point in the coastal zone, is described by the relationship:

$$\frac{1 - p_b}{\ln p_b} = - \left(\frac{H_{rms}}{H_m} \right)^2 \quad (3)$$

in which α is an empirical coefficient of the order $O(1)$, f_p is the wave spectrum peak frequency ($f_p = 1/T_p$), H_m denotes the maximum possible wave height at the considered location of the coastal zone, and H_{rms} is the sought-after root-mean-square wave height.

In the longshore sediment transport model, the following main assumptions are made:

- isobaths are approximately parallel to the shoreline,
- shear stresses within the liquid in the cross-shore direction play a predominant role,
- water flow velocities related to circulations of the open sea are negligibly small in comparison to wave-induced currents in the nearshore zone.

The time- and depth-averaged momentum equations in the cross-shore (x axis) and longshore (y axis) direction take the form:

$$\frac{\partial S_{xx}}{\partial x} + \frac{\partial M_{xx}}{\partial x} + \rho g h \frac{\partial \eta}{\partial x} = 0, \quad (4)$$

$$\frac{\partial S_{xy}}{\partial x} + \frac{\partial M_{xy}}{\partial x} = \frac{\partial \tau_{xy}}{\partial x} - \tau_{by}, \quad (5)$$

where η denotes the mean elevation of the free surface above the still water level, h the water depth, τ_{by} the bed shear stress, τ_{xy} the turbulence shear stresses within the liquid, S_{xx} and S_{xy} the components of the radiation stress tensor, M_{xx} and M_{xy} the components of the roller momentum tensor.

The above equations enable the set-up and set-down of sea water level (eq. (4)) and the distribution of longshore currents, averaged over depth and wave period, to be computed as functions of offshore distance (eq. (5)) above a multi-bar bottom and for multiple wave breaking.

The driving factors S_{xy} and M_{xy} of water flow are calculated as the function of wave energy dissipation:

$$\frac{\partial S_{xy}}{\partial x} = -\frac{\sin \theta}{C} D, \quad (6)$$

$$\frac{\partial M_{xy}}{\partial x} = \frac{\sin \theta}{C} (D - D_r), \quad (7)$$

where D_r is the wave energy dissipation due to the appearance of the roller.

The bed stress is calculated under the classical assumption of the relationship between the shear stresses at the top of the bed boundary layer and the flow velocities beyond this layer, whereas the turbulence stresses are expressed by the mean parameters of the flow in accordance with the Boussinesq hypothesis.

2.2. Asymmetric wave free-stream velocities

The ultimate effect of the nearbed interaction between asymmetric wave motion and wave-induced steady flow (e.g. longshore current) depends on the wave shape, in particular the shape of the wave free-stream velocity.

The most elementary description of asymmetric waves is provided by the classical Stokes theory. This approach, however, can only be used for a limited range of wave parameters. Close to the shore, at small water depths, the Stokes approximations are not valid. In this area, therefore, the application of the cnoidal wave theory is recommended.

Following conventional classifications, e.g. by Massel (1989), one can assume the rough limit of $L/h \approx 10$ as the interaction between short and long waves. The wave theories stemming from Stokes approximations can

be used for $L/h < 10$, whereas the theoretical approaches to long waves – cnoidal theories – should be used for $L/h > 10$. According to Fenton (1979), the above intersection lies at about $L/h = 8$. However, as deduced by Fenton (1979), for smaller waves there is significant overlap between the areas of validity of the Stokes and cnoidal theories. For instance, a wave with $H/h = 0.2$ can be solved using either the Stokes or the cnoidal approximation for L/h lying between 5 and 12. The above wave conditions yield an Ursell parameter, $U_r = H/h(L/h)^2$, ranging from 5 to 28.8. This example shows that an arbitrary choice can be made between the two theoretical approaches within quite a wide range of wave regimes.

Sobey et al. (1987) proposed the following formulas for the free surface elevation η and the horizontal depth-averaged velocity u (for the symbols, see Fig. 1):

$$\eta(x, t) = h_t + H \text{cn}^2(x, t, k), \quad (8)$$

$$u(x, t) = \bar{u} + (gh_t)^{1/2} \left[-1 - \frac{H}{h_t \text{cn}^2(x, t, k)} (-0.5 + k^2 - k^2 \text{cn}^2(x, t, k)) \right] \quad (9)$$

in which

$$h_t = h \left\{ 1 + \frac{H}{k^2 h} \left[1 - k^2 - \frac{\mathbf{E}(k)}{\mathbf{K}(k)} \right] \right\}, \quad (10)$$

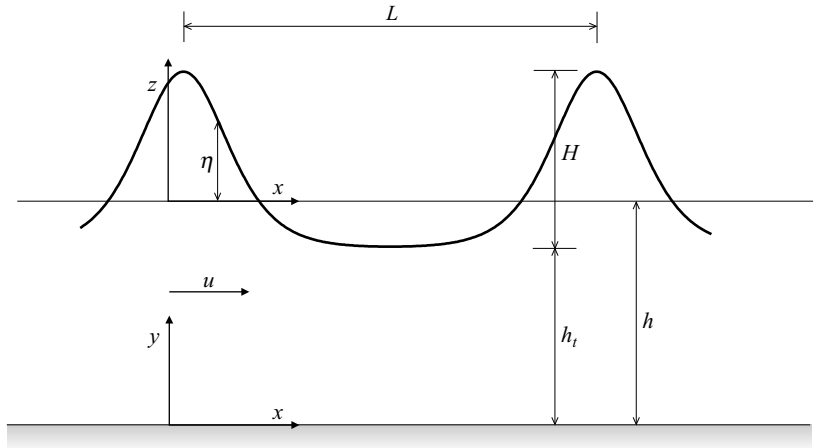


Fig. 1. Definition sketch for wave theories

$$\bar{u} = (gh_t)^{1/2} \left\{ 1 + \frac{H}{k^2 h_t} \left[0.5 - \frac{\mathbf{E}(k)}{\mathbf{K}(k)} \right] \right\}, \quad (11)$$

$$\text{cn}^2(x, t, k) = \text{cn}^2 \left[2\mathbf{K}(k) \left(\frac{x}{L} - \frac{t}{T} \right); k \right]. \quad (12)$$

In the above expressions, $\mathbf{K}(k)$ and $\mathbf{E}(k)$ are complete elliptic integrals of the first and second kind, respectively, with modulus k . Function ‘cn’ is the Jacobian elliptic cosine. The function ‘cn’ is singly periodic, provided k is a real number and $0 \leq k < 1$. The period becomes infinite when $k = 1$ (in which case we have a solitary wave). For $k = 0$ the wave is sinusoidal.

For the same as the above description of the free surface elevation, Wiegel (1960) provided a more sophisticated equation yielding the horizontal velocity u variable over the elevation y above the bed:

$$\begin{aligned} \frac{u(x, y, t)}{(gh)^{1/2}} = & -\frac{5}{4} + \frac{3h_t}{2h} - \frac{h_t^2}{4h^2} + \left(\frac{3h}{2h} - \frac{h_t H}{2h^2} \right) \text{cn}^2(x, t, k) - \\ & - \frac{H^2}{4h^2} \text{cn}^4(x, t, k) - \frac{8H\mathbf{K}^2(k)}{L^2} \left(\frac{h}{3} - \frac{y^2}{2h} \right) \left[-k^2 \text{sn}^2(x, t, k) \text{cn}^2(x, t, k) + \right. \\ & \left. + \text{cn}^2(x, t, k) \text{dn}^2(x, t, k) - \text{sn}^2(x, t, k) \text{dn}^2(x, t, k) \right], \end{aligned} \quad (13)$$

where ‘sn’ and ‘dn’ are the other two Jacobian elliptic functions (available on the basis of ‘cn’ from the relations $\text{sn}^2 + \text{cn}^2 = 1$ and $k^2 \text{sn}^2 + \text{dn}^2 = 1$).

In all the above and other solutions for cnoidal waves, the modulus k of the elliptic integrals, as well as the elliptic integrals $\mathbf{K}(k)$ and $\mathbf{E}(k)$ are unknown. In the present study, they are found iteratively from the following relationship, after Massel (1989):

$$\left(\frac{H}{h} \right) \left(\frac{gT^2}{h} \right) = \frac{16}{3} k^2 \mathbf{K}^2(k), \quad (14)$$

whereas the cnoidal wave length is calculated from the following equation (assuming the wave celerity $C = L/T = (gh)^{1/2}$):

$$\left(\frac{H}{h} \right) \left(\frac{L}{h} \right)^2 = \frac{16}{3} k^2 \mathbf{K}^2(k). \quad (15)$$

Where applicable, the Stokes theory can be applied in calculations of the free surface elevation η and the nearbed wave-induced velocity u . In case of the 2nd Stokes approximation, these quantities read (Massel 1992):

$$\eta(x, t) = \frac{H}{2} \cos \left[2\pi \left(\frac{x}{L} - \frac{t}{T} \right) \right] + \left(\frac{\pi H^2}{8L} \right) \frac{\cosh \left(\frac{2\pi h}{L} \right)}{\sinh^3 \left(\frac{2\pi h}{L} \right)} \left[2 + \cosh \left(\frac{4h}{L} \right) \right] \cos \left[4\pi \left(\frac{x}{L} - \frac{t}{T} \right) \right], \quad (16)$$

$$u(x, y, t) = \frac{gHT}{2L} \frac{\cosh \left(\frac{2\pi(z+h)}{L} \right)}{\cosh \left(\frac{2\pi h}{L} \right)} \cos \left[2\pi \left(\frac{x}{L} - \frac{t}{T} \right) \right] + \frac{3}{4} \left(\frac{\pi H}{L} \right)^2 C \frac{\cosh \left(\frac{4\pi(z+h)}{L} \right)}{\sinh^4 \left(\frac{2\pi h}{L} \right)} \cos \left[4\pi \left(\frac{x}{L} - \frac{t}{T} \right) \right]. \quad (17)$$

Example computations of the free surface elevation using eq. (8), the depth-independent velocity using eq. (9), the velocities at the bottom and in the wave trough using eq. (13), as well as the free surface elevation and nearbed velocity using the 2nd Stokes approximation from eqs. (16) and (17) respectively, are plotted in Fig. 2.

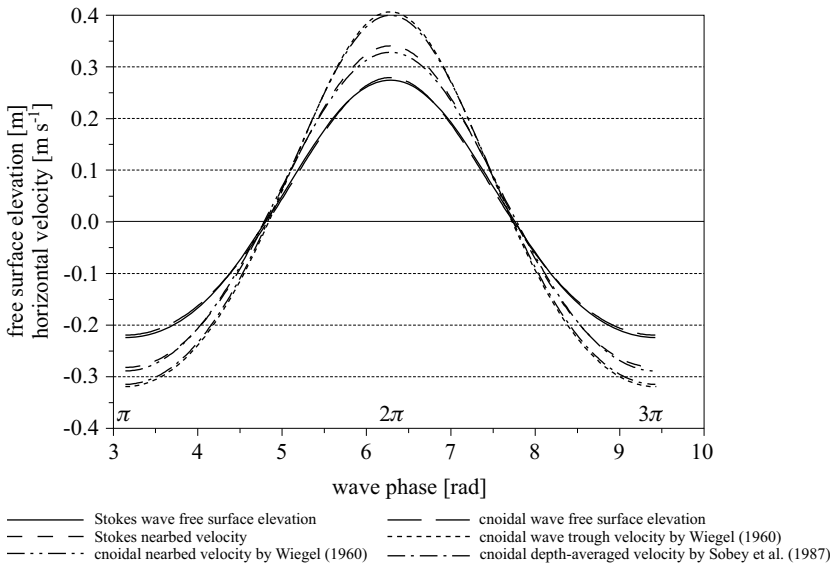


Fig. 2. Free surface elevation and wave-induced velocity by various approaches for $h = 5$ m, $H = 0.5$ m, $T = 8$ s; $L/h \approx 11$, $U_r \approx 11$

It can be seen that the cnoidal depth-averaged velocity computed from eq. (9) corresponds to the cnoidal velocity in the wave trough found from eq. (13), while the 2nd Stokes approximation yields a velocity almost identical with eq. (13) for $y = 0$ (nearbed velocity). The latter demonstrates that in the wave regime under consideration ($L/h \approx 11, U_r \approx 11$), both Wiegel's (1960) cnoidal approximation and Stokes' theory can be applied to describe nearbed wave-induced (free stream) velocities. For higher values of L/h and U_r , Wiegel's approach is recommended. More discussion on the above can be found in Ostrowski (2002).

2.3. Bed shear stresses and sediment transport

Longshore transport is assumed to depend on combined wave and current motion. This combined flow of water gives rise to a coupled bed shear stress, which is the force driving the movement of sand.

According to the assumptions of the present theoretical model, the motion of sediment is caused by the instantaneous bed shear stress ($\tau = \rho u_f^2$), where u_f is the friction velocity. The instantaneous values and directions during a wave period are determined by the momentum integral method for wave-current flow proposed by Fredsøe (1984). For the case of a wave and a steady current interacting at an arbitrary angle, Fredsøe (1984), using the dimensionless variable z_1 described as

$$z_1 = \frac{U\kappa}{u_f^*}, \quad (18)$$

derived the following differential equation:

$$\frac{d(z_1)}{d(\omega t)} = \frac{z_1(1+z_1-e^{z_1})}{e^{z_1}(z_1-1)+1} \frac{1}{U} \frac{dU}{d(\omega t)} + \frac{30\kappa}{k_e} \frac{\sqrt{\kappa^2 U^2 + z_1^2 u_{f0}^2 + 2z_1 \kappa u_{f0} U \cos \gamma}}{\omega [e^{z_1}(z_1-1)+1]}. \quad (19)$$

In the above equation, the input data consists of the von Karman constant $\kappa = 0.4$, the angular frequency ω of the wave motion, the free-stream velocity $U(\omega t)$, the friction velocity u_{f0} related to the steady flow (e.g. longshore current) at the top of the wave bed boundary layer, the angle between this flow (of the velocity $u_m(\delta)$ at the top of the bed boundary layer) and the direction of wave propagation γ (see Fig. 3), as well as the bed roughness height k_e . From the solution of eq. (19), the function $z_1(\omega t)$ is obtained, from which one can calculate the distribution of the boundary layer thickness $\delta(\omega t)$ over the wave period using eq. (20).

$$\delta = \frac{k_e}{30} (e^{z_1} - 1). \quad (20)$$

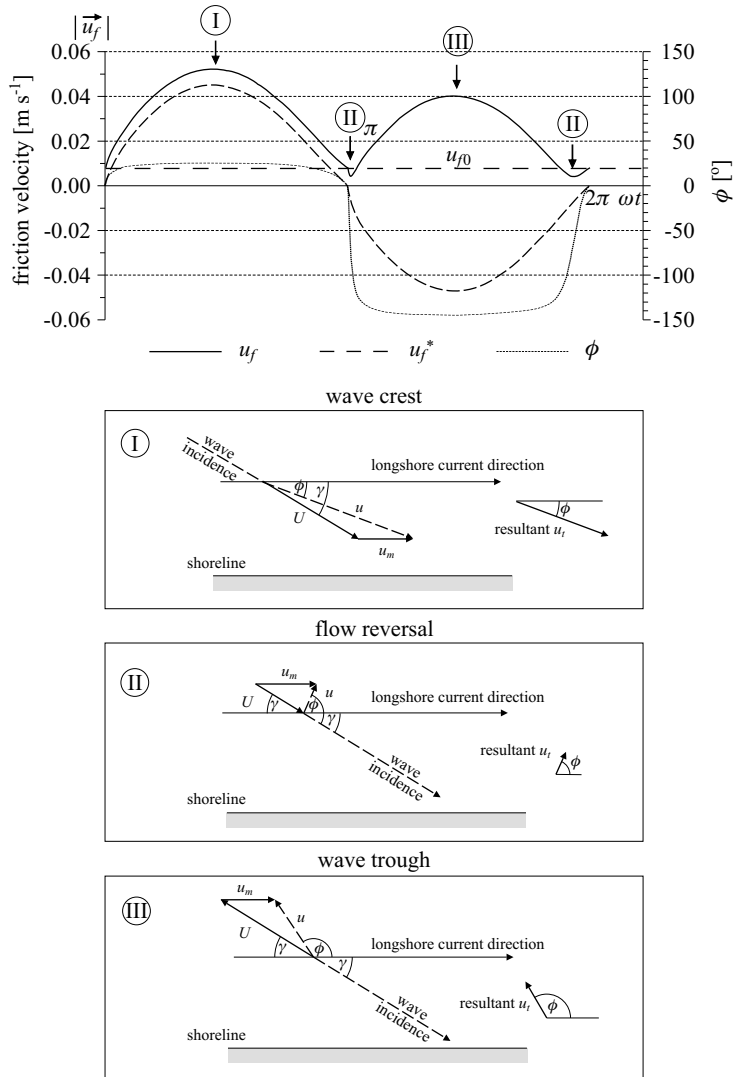


Fig. 3. Calculated friction velocities (upper) and schemes of interaction between waves and the longshore current in the bed boundary layer of the coastal zone

In accordance with Fredsøe’s (1984) approach, the distribution of the friction velocity $u_f(\omega t)$ is determined from the following equation, in which u_f^* is an auxiliary variable:

$$\frac{1}{u_f^*} = \frac{u_{f0} \cos \gamma}{u_f^2 - u_{f0}^2} + \sqrt{\frac{u_{f0}^2 \cos^2 \gamma}{(u_f^2 - u_{f0}^2)^2} + \frac{1}{u_f^2 - u_{f0}^2}}. \quad (21)$$

The angle $\phi(\omega t)$ between the direction of the steady current and the resultant instantaneous bed shear stress is calculated by the following formula:

$$\phi = \arcsin \left(\frac{u_f^*}{u_f} \sin \gamma \right). \quad (22)$$

The upper part of Fig. 3 exemplifies the results of the computations; the lower part shows the layout of velocity vectors together with the resultant friction velocity u_f during consecutive phases of the wave period.

The solution yields the instantaneous bed shear stresses $\tau = \rho u_f^2(\omega t)$ and the resultant directions of these stresses $\phi(\omega t)$.

The shear stresses are the forces driving sediment transport rates, which are determined using the model of Kaczmarek & Ostrowski (2002). Successful, thorough testing versus experimental data allow this model to be applied within the framework presented here.

The three-layer sediment transport model comprises the bedload layer (below the theoretical bed level) and two suspension layers – the contact load layer (nearbed suspension of sediment) and the outer layer (suspension in the water column).

The mathematical model of the bedload transport is based on the water-soil mixture approach, with a collision-dominated drag concept and the effective roughness height k_e (necessary for determining the bed shear stresses). This roughness is calculated using the approximate formula presented by Kaczmarek & Ostrowski (1996).

From the hydrodynamic input, described by the nearbed wave-induced velocities and the longshore current velocity, the instantaneous values of bed shear stresses $\rho u_f^2(t)$ during a wave period are determined by the momentum integral method proposed by Fredsøe (1984), i.e. from eq. (19). Then, for known bed shear stresses $\rho u_f^2(t)$, the instantaneous bedload velocities $u(z', t)$ and concentrations $c(z', t)$ are found from the following equations (with the vertical z' axis directed downwards from the theoretical bed level):

$$\alpha^0 \left(\frac{c - c_0}{c_m - c} \right) \sin \varphi \sin 2\Psi + \mu_1 \left(\frac{\partial u}{\partial z'} \right)^2 = \rho u_f^2, \quad (23)$$

$$\begin{aligned} & \alpha^0 \left(\frac{c - c_0}{c_m - c} \right) (1 - \sin \varphi \sin 2\Psi) + (\mu_0 + \mu_2) \left(\frac{\partial u}{\partial z'} \right)^2 = \\ & = \left(\frac{\mu_0 + \mu_2}{\mu_1} \right) \Big|_{c=c_0} \rho u_f^2 + (\rho_s - \rho) g \int_0^{z'} c dz', \end{aligned} \quad (24)$$

where

ρ_s – is the soil density,

α^0 – is a constant,

c_0 – is the sediment concentration corresponding to soil fluidity,

c_m – is the sediment concentration corresponding the closest possible packing of grains,

μ_0, μ_1 and μ_2 – are functions of the solid concentration c :

$$\frac{\mu_1}{\rho_s d^2} = \frac{0.03}{(c_m - c)^{1.5}}, \quad (25)$$

$$\frac{\mu_0 + \mu_2}{\rho_s d^2} = \frac{0.02}{(c_m - c)^{1.75}}, \quad (26)$$

where d is the grain diameter.

The symbol φ in equations (23) and (24) stands for the quasi-static angle of internal friction, and the angle ψ between the major principal stress and the horizontal axis (for simple shear flow) is equal to

$$\Psi = \frac{\pi}{4} - \frac{\varphi}{2}. \quad (27)$$

The following numerical values are assumed in the calculations:

$$\frac{\alpha^0}{\rho_s g d} = 1 \quad c_m = 0.53 \quad c_0 = 0.32 \quad \varphi = 24.4^\circ. \quad (28)$$

In the contact load layer, following Deigaard (1993), the sediment velocity and concentration is modelled using the following equations (with the vertical z axis directed upwards from the theoretical bed level):

$$\left[\frac{3}{2} \left(\alpha \frac{d}{w_s} \frac{du}{dz} \frac{2s + c_M}{3 c_D} + \beta \right)^2 d^2 c^2 (s + c_M) + l^2 \right] \left(\frac{du}{dz} \right)^2 = u_f'^2, \quad (29)$$

$$\left[3 \left(\alpha \frac{d}{w_s} \frac{du}{dz} \frac{2s + c_M}{3 c_D} + \beta \right)^2 d^2 \frac{du}{dz} c + l^2 \frac{du}{dz} \right] \frac{dc}{dz} = -w_s c. \quad (30)$$

The term $\rho u_f'^2(\omega t)$ is related to the 'skin friction', calculated by Fredsøe's (1984) model for the 'skin' roughness $k_e' = 2.5d$. In equations (29) and (30) w_s denotes the settling velocity of grains, c_M and c_D are the respective added mass and drag coefficients, α and β are the coefficients, and l is the mixing length defined as $l = \kappa z$.

The instantaneous values of the sediment transport rate are computed from the distributions of velocity and concentration in the bedload layer and in the contact load layer:

$$q_{b+c}(t) = \int_0^{\delta_b} u(z', t) c(z', t) dz' + \int_{k_e'/30}^{\delta_c} u(z, t) c(z, t) dz, \quad (31)$$

where $\delta_b(\omega t)$ is the bedload layer thickness, and δ_c denotes the upper limit of the nearbed suspension (contact load layer thickness). The quantity δ_b results from the solution of eqs. (23) and (24), and the value of δ_c is the characteristic boundary layer thickness calculated on the basis of Fredsøe's (1984) approach (see Kaczmarek & Ostrowski 2002).

The net transport rate in the bedload and contact load layers is calculated as follows:

$$q_b + q_c = \frac{1}{T} \int_0^T q_{b+c}(t) dt. \quad (32)$$

The net sediment transport rate in the outer flow is determined using the following simplified formula:

$$q_s = \int_{\delta_c}^h \bar{u}(z) \bar{c}(z) dz, \quad (33)$$

where the time-averaged concentration is obtained from a conventional relationship, e.g. that by Ribberink & Al-Salem (1994):

$$\bar{c}(z) = \bar{c}(z = \delta_c) \left(\frac{\delta_c}{z} \right)^{\alpha_1}. \quad (34)$$

The quantity $\bar{c}(z = \delta_c)$ in eq. (34) plays a key role in the determination of concentration in the outer region. Known as a reference concentration, it is assumed arbitrarily, assessed from experimental data or simply 'guessed' in the other theoretical approaches. In the present modelling system, the concentration $\bar{c}(z = \delta_c)$ is calculated from eqs. (29) and (30), whereas the velocity $\bar{u}(z)$ is determined from the solution of the bed boundary layer presented by Kaczmarek & Ostrowski (1992). Beyond the bed boundary layer in the water column the velocity $\bar{u}(z)$ is assumed to be the constant quantity. The concentration decay parameter α_1 is an unknown value which has to be determined, e.g. from experiments.

Next, using the angle ϕ , the instantaneous sediment transport rates $q(\omega t)$ are projected on to the longshore direction, averaged over the wave period; thus, the net longshore transport q_y is obtained:

$$q_y = \overline{q(\omega t) \cos \phi(\omega t)}. \quad (35)$$

The inner time-averaged velocity profiles in the bed boundary layer (discussed by Kaczmarek & Ostrowski (1992) and assumed to lie within $z < 2\delta_m + k_e/30$) in the direction of the steady current can be determined using the formulas proposed by Kaczmarek & Ostrowski (1992):

$$\bar{u}(z) = \frac{u_{fc}^2}{\kappa \hat{u}_f} \ln \frac{30z}{k_e} \quad \text{for} \quad \frac{k_e}{30} < z < \frac{\delta_m}{4} + \frac{k_e}{30}, \quad (36)$$

$$\bar{u}(z) = \frac{u_{fc}^2}{\kappa \hat{u}_f} \left(\frac{z}{\frac{\delta_m}{4} + \frac{k_e}{30}} + \ln \frac{\frac{\delta_m}{4} + \frac{k_e}{30}}{\frac{k_e}{30}} - 1 \right)$$

for $\frac{\delta_m}{4} + \frac{k_e}{30} < z < 2\delta_m + \frac{k_e}{30}$. (37)

The above relationships are completed as follows (notation similar to Fredsøe 1984):

$$\hat{u}_f = \max[|u_f(\omega t)|], \quad (38)$$

$$\delta_m = \max(\delta_1, \delta_2), \quad (39)$$

$$u_{fc} = \sqrt{\frac{1}{T} \int_0^T |u_f(t)| u_f(t) \cos \phi(t) dt}, \quad (40)$$

where δ_1 and δ_2 are the thicknesses of the bed boundary layer $\delta(\omega t)$ at the moments corresponding to the respective extreme positive and negative resultant (wave-current) flow velocities at the top of the bed boundary layer.

The mean velocity in the outer region is known from the theoretical solution for wave transformation and wave-driven currents, described in section 2.1. An iterative procedure should be applied, by which the quantity u_{f_0} (unknown in eq. (19)) can be found. A scheme for the iterative procedure was proposed by Ostrowski (2004). Knowing u_{f_0} , one can determine from eq. (19) the instantaneous value and direction of the shear stress $\rho u_f^2(\omega t)$, which is the force driving sediment transport.

3. Results and discussion

The model was run for a typical bathymetric cross-shore profile measured at CRS Lubiatowo. Some 1100 m long and more than 9 m deep on its offshore boundary, the profile comprised the entire coastal zone, with 4 distinct bars, as shown in Fig. 4c. The offshore wave parameters used in the model were as follows: root-mean-square wave height $H_{rms} = 1.5$ m, wave period corresponding to maximum energy (wave peak period) $T_p = 6$ s

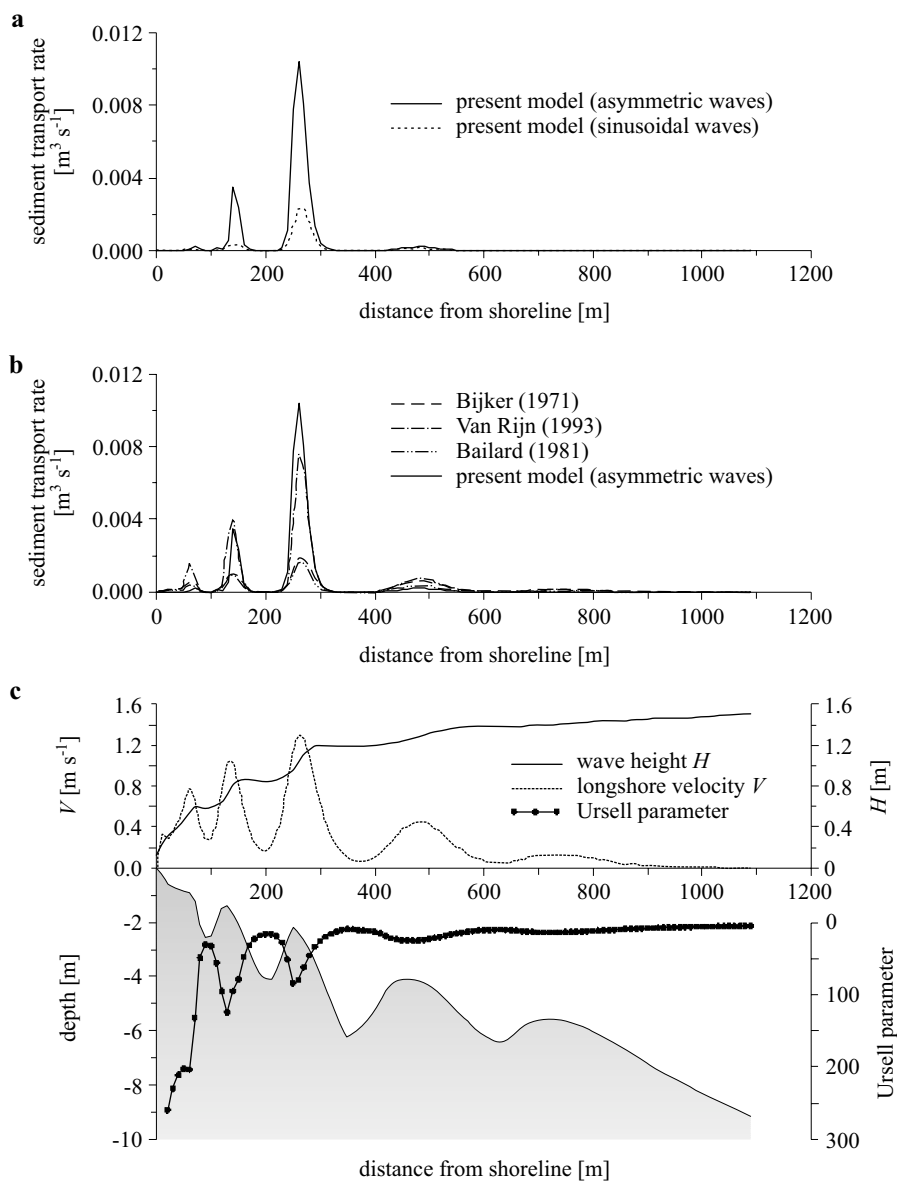


Fig. 4. Cross-shore sea bed profile at CRS Lubiatoowo with wave heights, longshore flow velocities and Ursell numbers calculated for incipient wave parameters: $H_{rms} = 1.5$ m, $T_p = 6$ s and $\theta = 45^\circ$ (c); longshore sediment transport rate distribution over the cross-shore profile at CRS Lubiatoowo determined by the present modelling system and the models of Bailard (1981), Bijker (1971) and Van Rijn (1993) (b); distributions of longshore sediment transport rates over the cross-shore profile at CRS Lubiatoowo determined by the present modelling system for sinusoidal and asymmetric waves (a)

and wave approach angle (angle between the wave ray and the cross-shore direction) $\theta = 45^\circ$. Such parameters correspond to typical winter storm conditions on the southern Baltic coast. The hydrodynamic outputs of the model, i.e. wave height variability and longshore flow velocity on the cross-shore profile, together with the distribution of the Ursell parameter, are also shown in Fig. 4c.

The median grain size diameter was assumed to be $d_{50} = 0.22$ mm (with fall velocity $w_s = 2.5$ cm s⁻¹), in accordance with actual sediment sampled at the Lubiatowo site. The distribution of longshore sediment transport rates on the cross-shore transect, determined by the present modelling system for asymmetric waves, is illustrated in Fig. 4b. The concentration decay parameter $\alpha_1 = 2.1$ was used in computations of sediment transport rates above the bed. For comparison, the rates determined (using the same hydrodynamic forcing) by the sediment transport models of Bailard (1981), Bijker (1971) and Van Rijn (1993) are also plotted in Fig. 4b.

It can be seen from the plots of Fig. 4b that the present modelling results lie below the other solutions presented, except for the locations 230–310 m offshore (at the second bar), where the present model for asymmetric waves gives the highest rates. At the other cross-shore locations, Van Rijn's (1993) approach yields higher rates than all the other models.

In order to assess the influence of wave asymmetry on sediment transport rates, the results for sinusoidal and asymmetric waves are presented in Fig. 4a; this shows clearly that an asymmetric wave shape leads to significant growth in sediment transport.

In coastal engineering practice, the detailed distribution of the longshore sediment transport rate on the cross-shore profile is not as important as the total (global) sediment transport rate in the longshore direction. This quantity is particularly significant in calculations of shoreline evolution using the one-line theory, in which shoreline advance or retreat depends on the spatial variability of the total longshore sediment transport rates (integrated over the cross-shore transect).

Therefore, for an ultimate assessment of the results, the computational data integrated over the cross-shore profile are given in Table 1, in which the present model output is shown, together with the quantities obtained using conventional theoretical models. In addition, Table 1 shows the results obtained with the well-known CERC 'global' sediment transport model (see Shore Protection Manual 1977).

Table 1 shows that the present model result for asymmetric waves lies between the solution by the CERC formula and the result of Van Rijn's (1993) model. At the same time, it is higher than the results obtained

Table 1. Total longshore sediment transport rates by the present approach and the models of Bailard (1981), Bijker (1971) and Van Rijn (1993)

Approach	Present model		Bailard (1981)	Bijker (1971)	Van Rijn (1993)	CERC
	asymmetric waves	sinusoidal waves				
rate [m ³ s ⁻¹]	0.426	0.114	0.151	0.228	0.464	0.376

with Bailard's (1981) and Bijker's (1971) models. The present model for sinusoidal waves yields a very low value, smaller than all the other results.

On the basis of Table 1, it can be concluded that the present modelling system does provide an accurate prediction of longshore sediment transport rates. Nevertheless, this is not clearly confirmed by detailed graphical inspection of the computational results in Fig. 4, which reveals a highly nonlinear relationship between the hydrodynamic input (Fig. 4c) and the sediment transport rates (Fig. 4b). The results obtained with all the models considered here show that most of the longshore sediment transport is concentrated in a relatively narrow zone near the major wave breaker, where high waves are accompanied by a strong longshore flow. The present model very distinctly highlights this effect.

It should be pointed out that the results obtained with the present three-layer model do not depend on any parameters for bedload or contact (transitional) load. Only sediment transport rates in the outer region can be 'tuned' slightly, by modifying the concentration decay parameter α_1 . The present approach is thus more unbiased than the other models, the results of which depend on a number of arbitrarily assumed coefficients and parameters.

References

- Bailard J. A., 1981, *An energetics total load sediment transport model for a plane sloping beach*, J. Geophys. Res., 86 (C11), 10938–10954.
- Battjes J. A., Janssen J. P. F. M., 1978, *Energy loss and set-up due to breaking of random waves*, Proc. 16th ICCE, Vol. 1, 569–587.
- Bijker E. W., 1971, *Longshore transport computations*, J. Waterway. Harbour. Coast. Eng. Div.-ASCE, 97 (WW4), 687–701.
- Deigaard R., 1993, *Modelling of sheet flow: dispersion stresses vs. the diffusion concept*, Prog. Rep. 74, Inst. Hydrodyn. Hydraul. Eng., Tech. Univ. Denmark, 65–81.
- Fenton J. D., *A high-order cnoidal wave theory*, Part 1, J. Fluid Mech., 94, 129–161.
- Fredsøe J., 1984, *Turbulent boundary layer in combined wave-current motion*, J. Hydraul. Eng.-ASCE, 110 (HY8), 1103–1120.

- Kaczmarek L. M., Ostrowski R., 1992, *Modelling of wave-current boundary layer in the coastal zone*, Proc. 23rd ICCE, ASCE, New York, 350–363.
- Kaczmarek L. M., Ostrowski R., 1996, *Asymmetric and irregular wave effects on bedload: theory versus laboratory and field experiments*, Proc. 25th ICCE, ASCE, New York, 3467–3480.
- Kaczmarek L. M., Ostrowski R., 2002, *Modelling intensive near-bed sand transport under wave-current flow versus laboratory and field data*, Coast. Eng., 45 (1), 1–18.
- Massel S. R., 1989, *Hydrodynamics of coastal zones*, Elsevier, Amsterdam, 336 pp.
- Massel S. R., 1992, *Wave motion at open waters and limited aquatories*, [in:] *Poradnik hydrotechnika*, Wyd. Mor., Gdańsk, 338 pp., (in Polish).
- Ostrowski R., 2002, *Application of cnoidal wave theory in modelling of sediment transport*, Arch. Hydro-Eng. Environ. Mech., 49 (1), 107–118.
- Ostrowski R., 2003, *A quasi phase-resolving model of net sand transport and short-term cross-shore profile evolution*, Oceanologia, 45 (2), 261–282.
- Ostrowski R., 2004, *Morphodynamics of a multi-bar coastal zone*, IBW PAN, Gdańsk, 163 pp.
- Ribberink J. S., Al-Salem A., 1994, *Sediment transport in oscillatory boundary layers in cases of rippled beds and sheet flow*, J. Geoph. Res., 99 (C6), 12707–12727.
- Shore Protection Manual, 1977, US Army Coast. Eng. Res. Center.
- Sobey R. J., Goodwin P., Thieke R. J., Westberg R. J., 1987, *Application of Stokes, cnoidal and Fourier wave theories*, J. Waterw. Port C. Div., 113 (6), 565–587.
- Svendsen I. A., 1984, *Mass flux and undertow in a surf zone*, Coast. Eng., 8 (4), 347–365.
- Szmytkiewicz M., 1995, *2D velocity distributions in nearshore currents*, Proc. Coast. Dynam. '95, ASCE, New York, 366–376.
- Szmytkiewicz M., 2002a, *Quasi 3D model of wave-induced currents in coastal zone*, Archiv. Hydro-Eng. Environ. Mech., 49 (1), 57–81.
- Szmytkiewicz M., 2002b, *Wave-induced currents in the coastal zone*, IBW PAN, Gdańsk, 235 pp., (in Polish).
- Szmytkiewicz M., Biegowski J., Kaczmarek L. M., Okrój T., Ostrowski R., Pruszek Z., Różyński G., Skaja M., 2000, *Coastline changes nearby harbour structures: comparative analysis of one-line models versus field data*, Coast. Eng., 40 (2), 119–139.
- Van Rijn L. C., 1993, *Principles of sediment transport in rivers, estuaries and coastal seas*, Aqua Publ., Amsterdam, 614 pp.
- Wiegel R. L., 1960, *A presentation of cnoidal wave theory for practical application*, J. Fluid Mech., 7, 273–286.